

## Thermodynamic characterization of ferric and ferrous haem binding to a designed four- $\alpha$ -helix protein

Charles J. Reedy, Michelle L. Kennedy and Brian R. Gibney\*

Columbia University, Department of Chemistry, 3000 Broadway MC 3121, New York, NY 10027, USA.

E-mail: brg@chem.columbia.edu; Fax: +1 212 932 1289; Tel: +1 212 854 6346

Received (in Purdue, IN, USA) 20th November 2002, Accepted 24th January 2003

First published as an Advance Article on the web 10th February 2003

**The thermodynamics of ferric and ferrous haem affinity of a *de novo* designed four- $\alpha$ -helix bundle protein and the associated haem electrochemistry is described.**

The *de novo* design and redesign of metalloproteins is an area of intense research focused on elucidating the structure–function relationships of natural enzymes.<sup>1</sup> These constructive protein design approaches have afforded a variety of novel metalloproteins as model complexes for natural proteins involved in biological electron transfer, catalysis and gene regulation.<sup>2</sup> In particular, designed haem proteins have shown their utility in revealing key aspects of natural haem protein engineering including electrochemical function.<sup>3</sup>

Recently, Shifman *et al.*<sup>4</sup> have delineated the types and relative magnitudes of the various factors that affect haem reduction potentials within a designed four helix bundle protein scaffold, a haem protein maquette. Using the factors alone and in combination, the haem reduction potential in the maquette could be modulated by up to 435 mV (10.3 kcal mol<sup>-1</sup>), *nearly half the range observed for natural haem proteins*. Furthermore, the observed range encompasses the midpoint reduction potentials of the majority of designed haem proteins.<sup>3</sup> However, haem affinity data was only collected in the oxidized state, so conclusions about the relative stabilization/destabilization of the ferric and ferrous haems could not be made.

Since metalloproteins are highly elaborated coordination complexes,<sup>5</sup> we are interested in delineating the fundamental coordination equilibria of both Fe(III) and Fe(II) haems binding to designed protein scaffolds to understand the relative stabilization/destabilization of the haem oxidation states. The measurement of oxidized and reduced haem affinities coupled with the related haem electrochemistry is critical to understanding of how proteins control haem redox function.

The designed primary structure of each helix of the peptide ligand, [ $\Delta 7$ -H<sub>10</sub>I<sub>14</sub>I<sub>21</sub>]<sub>2</sub> (Ac-CGGGEIWLK·HEEFIKK·FEERIKK·L-CONH<sub>2</sub>), contains a single histidine per helix at position 10 (heptad *a*). An N-terminal cystine disulfide links the helices into a di- $\alpha$ -helical subunit which self-assembles as a non-covalent dimer, a four- $\alpha$ -helix bundle. The data demonstrate [ $\Delta 7$ -H<sub>10</sub>I<sub>14</sub>I<sub>21</sub>]<sub>2</sub> binds two Fe(III) or Fe(II)(protoporphyrin IX) cofactors, haem, *via* bis-histidine ligation as designed. Elucidation of the fundamental coordination chemistry thermodynamics of this designed protein reveals that the intrinsic affinity of histidine for Fe(III) and Fe(II) as well as haem macrocycle steric hinderance play a significant roles in establishing haem protein redox function.

The solution oligomerization state of the [ $\Delta 7$ -H<sub>10</sub>I<sub>14</sub>I<sub>21</sub>]<sub>2</sub> peptide ligand was evaluated using both FPLC size exclusion chromatography and sedimentation equilibrium analytical ultracentrifugation. Both techniques demonstrate that the protein exists as a single species in solution with a molecular weight consistent with a dimer in solution (pH 8, 20 mM KP<sub>i</sub>, 100 mM KCl, 1–30  $\mu$ M peptide). Furthermore, analytical ultracentrifugation demonstrates that haem incorporation does not alter the solution aggregation state.

The secondary structure and global folding stability of the protein scaffold was probed using circular dichroism spectroscopy.<sup>7</sup> The [ $\Delta 7$ -H<sub>10</sub>I<sub>14</sub>I<sub>21</sub>]<sub>2</sub> scaffold has minima at 222 and 208

nm consistent with the designed helical secondary structure.<sup>6</sup> The calculated helical content, 67% helix based on  $\Theta_{222}$ , is uniform between pH 3.5 and 11. Isothermal chemical denaturation studies using guanidine hydrochloride as a chaotropic agent demonstrate [ $\Delta 7$ -H<sub>10</sub>I<sub>14</sub>I<sub>21</sub>]<sub>2</sub> is stable in the apo-form,  $-\Delta G^{\text{H}_2\text{O}} = 11.4$  kcal mol<sup>-1</sup> at 298K ([Gdn-HCl]<sub>1/2</sub> value of 1.7 M; *m* value of 2.3). Thus, the protein exists as a stable four- $\alpha$ -helix bundle in solution, as designed.

Standard literature methods were used to incorporate two haems into the [ $\Delta 7$ -H<sub>10</sub>I<sub>14</sub>I<sub>21</sub>]<sub>2</sub> peptide ligand.<sup>3</sup> Fig. 1 shows the UV-visible spectrum of the [Fe(III) haem- $\Delta 7$ -H<sub>10</sub>I<sub>14</sub>I<sub>21</sub>]<sub>2</sub> complex ( $\lambda_{\text{max}}$  at 412 nm;  $\epsilon$  of 131,000 M<sup>-1</sup> cm<sup>-1</sup>) which is similar to other designed bis-histidine ligated haem proteins.<sup>3</sup> Haem reduction by sodium dithionite results in a shift in the Soret maximum to 427 nm ( $\epsilon$  of 209,000 M<sup>-1</sup> cm<sup>-1</sup>) and resolution of the  $\alpha/\beta$  bands at 559 and 528 nm ( $\epsilon$  of 28,000 and 16,000 M<sup>-1</sup> cm<sup>-1</sup>) which are indicative of bis-histidine ligation. Thus, the designed haem protein possesses UV-visible spectroscopic characteristics similar to bis-histidine ligated mammalian cytochrome b<sub>5</sub>.<sup>7</sup>

Fig. 1 also shows the electrochemistry of mono- and dihaem [ $\Delta 7$ -H<sub>10</sub>I<sub>14</sub>I<sub>21</sub>]<sub>2</sub> evaluated using redox potentiometric titrations. With a single haem incorporated into the four helix bundle, the equilibrium midpoint reduction potential of the haem is  $-222$  mV vs. SHE. The midpoint reduction potential is close to the  $-235$  mV reduction potential observed for bis-imidazole ligated haem in aqueous solution. Thus, by coincidence, the

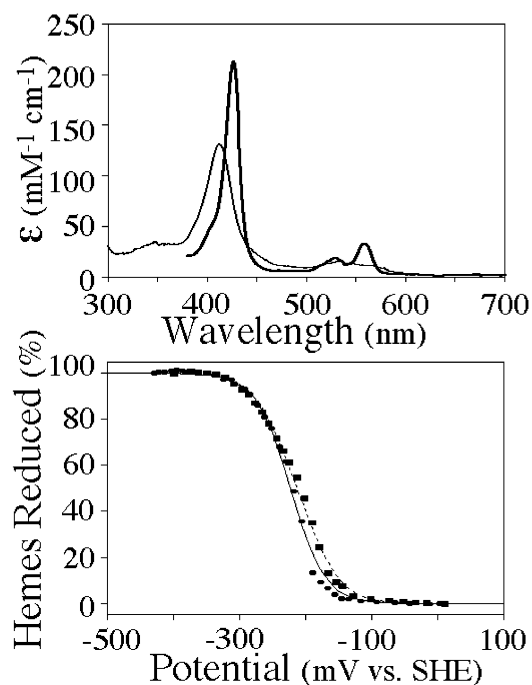


**Fig. 1** (Top) The oxidized and reduced (bold) haem optical spectra of [ $\Delta 7$ -H<sub>10</sub>I<sub>14</sub>I<sub>21</sub>]<sub>2</sub>. (Bottom) Comparison of the electrochemistry of [ $\Delta 7$ -H<sub>10</sub>I<sub>14</sub>I<sub>21</sub>]<sub>2</sub> in the mono- (circles, solid line) and dihaem (squares, dashed line) states.

various protein factors modulating the haem reduction potential sum to near zero. In the dihaem state, the electrochemistry demonstrates two  $N = 1$  midpoint potentials separated by 50 mV,  $-188$  mV and  $-238$  mV. As in previous haem protein maquettes,<sup>8</sup> we ascribe this 50 mV ( $1.2$  kcal mol<sup>-1</sup>), difference to haem–haem electrostatic interactions within the bundle's low dielectric hydrophobic core. The observation of haem–haem electrochemical interaction is consistent with a bundle in the *syn* topology, loop regions on the same side of the bundle with haem sites juxtaposed as shown in Scheme 1.

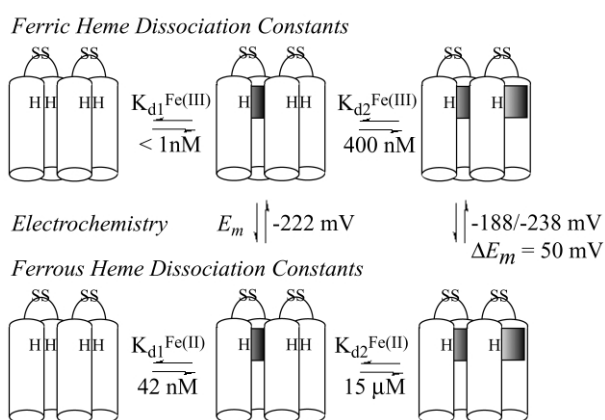
To fully describe the coordination chemistry thermodynamics of the four- $\alpha$ -helix bundle ligand, the oxidized and reduced state haem affinities were measured. The thermodynamic affinity of  $[\Delta 7\text{-H}_{10}\text{I}_{14}\text{I}_{21}]_2$  for ferrous haem was determined by anaerobic equilibrium titrations followed by UV-visible spectroscopy as shown in Fig. 2. The data demonstrate that the first haem binds tightly with a dissociation constant,  $K_{d1}^{\text{Fe(II)}}$ , value of 42 nM. The second ferrous haem binds significantly weaker than the first with an evaluated dissociation constant,  $K_{d2}^{\text{Fe(II)}}$ , value of 15  $\mu\text{M}$ . Since ferrous haems are formally neutral, we ascribe the observed 357-fold ( $3.5$  kcal mol<sup>-1</sup>) difference between the first and second Fe(II) haem affinities to steric hinderance in to the *syn* topology of the four helix bundle.

UV-visible titrations were also used to delineate the thermodynamic affinity of  $[\Delta 7\text{-H}_{10}\text{I}_{14}\text{I}_{21}]_2$  for ferric haem. Freshly prepared haemin solutions in DMSO were used to minimize the effects of haem aggregation.<sup>9</sup> The first ferric haem dissociation constant,  $K_{d1}^{\text{Fe(III)}}$ , was too tight to be measured,  $< 1$  nM. Comparison of the upper limit of  $K_{d1}^{\text{Fe(III)}}$  with the measured  $K_{d1}^{\text{Fe(II)}}$  value indicates that the bis-histidine site is binding Fe(III) tighter than Fe(II) despite the energetic penalty for the burial of the formal charged ferric haem within a low dielectric

hydrophobic core. The data are fully consistent with the inherent affinity of imidazole for Fe(III) over Fe(II) observed in iron porphyrins in organic solvents<sup>10</sup> and smaller designed haem protein models.<sup>11</sup> Thus, the data indicate that the metal–ligand interaction is overriding the penalty for burial of the formally charged  $[\text{Fe(III)(haem)}]^+$ . As observed for the ferrous haems, the second ferric haem binds weaker than the first with an evaluated dissociation constant,  $K_{d2}^{\text{Fe(III)}}$ , value of 400 nM. The corresponding  $> 400$ -fold difference in the  $K_{d1}^{\text{Fe(III)}}$  and  $K_{d2}^{\text{Fe(III)}}$  values includes the steric effect observed in the ferrous state ( $3.5$  kcal mol<sup>-1</sup>) as well as the observed 50 mV ( $1.2$  kcal mol<sup>-1</sup>) haem–haem electrostatic interaction which further weakens the affinity for the second oxidized haem. In fact, adding the  $1.2$  kcal mol<sup>-1</sup> electrostatic effect to the  $3.5$  kcal mol<sup>-1</sup> steric effect suggests that the ratio of the oxidized haem dissociation constants should be  $\approx 2900$  ( $4.7$  kcal mol<sup>-1</sup>) which places  $K_{d1}^{\text{Fe(III)}}$  at  $\approx 140$  pM. Thus, the estimated  $K_{d1}^{\text{Fe(III)}}$  value is tighter than any other *de novo* designed haem protein and approaches the 4 pM value for ferric cytochrome *b*<sub>5</sub>, a natural bis-histidine ligated haem protein.<sup>7</sup>

In conclusion, the detailed thermodynamic analysis presented in Scheme 1 reveals insight into the relative roles of ligand preference, steric hinderance and haem–haem electrostatic repulsion in haem protein design. First, the inherent preference of histidine for Fe(III) over Fe(II) can outweigh the energetic cost of oxidized haem burial. Second, the major contributor to weaker binding of the second oxidized or reduced haem is sterics rather than electrostatics. Thus, these data clearly underscore the importance of determining the metal ion affinity in each oxidation state along with the corresponding electrochemistry in developing a full understanding of the designed metalloprotein. Studies are underway to determine the oxidized and reduced haem affinities and electrochemistry of designed haem proteins with altered midpoint reduction potentials aimed at controlling the Fe(III) and Fe(II) haem affinities and, hence, redox activities.

We thank the National Science Foundation (CHE-02-12884) for financial support of this research. C.J.R. is a National Institutes of Health trainee (T32 GM08281).



**Scheme 1** Thermodynamic cycle of haem binding and electrochemistry.

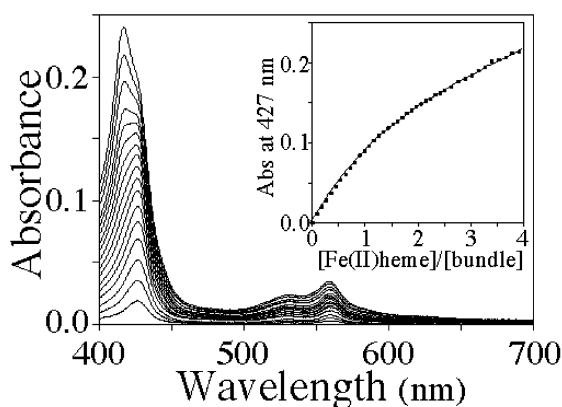


**Fig. 2** Spectrometric titration determination of  $K_{d1}^{\text{Fe(II)}}$ .

## Notes and references

- Y. Lu, S. M. Berry and T. D. Pfister, *Chem. Rev.*, 2001, **101**, 3047; M. L. Kennedy and B. R. Gibney, *Curr. Opin. Chem. Biol.*, 2001, **11**, 485; W. F. DeGrado, C. M. Summa, V. Pavone, F. Natri and A. Lombardi, *Annu. Rev. Biochem.*, 1999, **68**, 779.
- D. E. Robertson, R. S. Farid, C. C. Moser, J. L. Urbauer, S. E. Mulholland, R. Pidikiti, J. D. Lear, A. J. Wand, W. F. DeGrado and P. L. Dutton, *Nature*, 1994, **368**, 425; D. E. Benson, M. S. Wisz and H. W. Hellinga, *Proc. Natl. Acad. Sci. USA*, 2000, **97**, 6292; J. T. Welch, M. Sirish, K. M. Lindstrom and S. J. Franklin, *Inorg. Chem.*, 2001, **40**, 1982; B. T. Farrer, N. P. Harris, K. E. Balchus and V. L. Pecoraro, *Biochemistry*, 2001, **40**, 14696.
- B. R. Gibney and P. L. Dutton, in *Adv. Inorg. Chem.*, eds. A. G. Mauk and A. G. Sykes, Academic Press, NY, 2001, vol. 51, 409; A. Lombardi, F. Natri and V. Pavone, *Chem. Rev.*, 2001, **101**, 3165.
- J. M. Shifman, B. R. Gibney, R. E. Sharp and P. L. Dutton, *Biochemistry*, 2000, **39**, 14813.
- R. H. Holm and J. A. Ibers, *Science*, 1980, **209**, 223.
- K. Nakanishi, N. Berova and R. W. Woody, *Circular dichroism of peptides*, VCH, New York, NY, 1994, pp. 570.
- L. D. Gruenke, J. Sun, T. M. Loehr and L. Waskell, *Biochemistry*, 1997, **36**, 7114.
- A. M. Grosset, B. R. Gibney, F. Rabanal, C. C. Moser and P. L. Dutton, *Biochemistry*, 2001, **40**, 5474.
- S. B. Brown, T. C. Dean and P. Jones, *Biochem. J.*, 1970, **117**, 733–739.
- N. J. M. Nasset, N. V. Shokhirev, P. D. Enemark, S. E. Jacobson and F. A. Walker, *Inorg. Chem.*, 1996, **35**, 5188.
- M. L. Kennedy, S. Silchenko, N. Houndonougbo, B. R. Gibney, P. L. Dutton, K. S. Rodgers and D. R. Benson, *J. Am. Chem. Soc.*, 2001, **123**, 4635.